

Short Note

5-Vinyl-1*H*-tetrazole

Daria M. Krygina ¹, Eugene V. Sivtsov ², Yuliya N. Pavlyukova ³, Ekaterina N. Chernova ⁴ ,
 Mariya A. Skryl'nikova ^{3,5}, Vadim A. Baigildin ⁶, Aleksandra M. Puzyk ⁷ , Alexander A. Oskorbyn ²,
 Rostislav E. Trifonov ³, Pavel A. Aleshunin ³ and Vladimir A. Ostrovskii ^{3,4,*} 

- ¹ Laboratory of Polymer Sorbents and Carriers for Biotechnology, Institute of Macromolecular Compounds, Russian Academy of Sciences (IMC RAS), 31 Bolshoy Prospekt V.O., 199004 St. Petersburg, Russia
- ² Department of Physical Chemistry, Saint Petersburg State Institute of Technology, 24–26/49 Moskovsky Ave., 190013 St. Petersburg, Russia
- ³ Department of Chemistry and Technology of Nitrogen-Containing Organic Compounds, Saint Petersburg State Institute of Technology, 24–26/49 Moskovsky Ave., 190013 St. Petersburg, Russia
- ⁴ Saint Petersburg Federal Research Center, Russian Academy of Sciences (SPC RAS), 39, 14th Line, 199178 St. Petersburg, Russia
- ⁵ Department of Organic Chemistry, Saint Petersburg State Institute of Technology, 24–26/49 Moskovsky Ave., 190013 St. Petersburg, Russia
- ⁶ Department of General and Inorganic Chemistry, Institute of Chemistry, Saint Petersburg State University, 26 Universitetskii Prospekt, Petergof, 198504 St. Petersburg, Russia
- ⁷ Research Park, Saint Petersburg State University, 26 Universitetskii Prospekt, Petergof, 198504 St. Petersburg, Russia
- * Correspondence: va_ostrovskii@mail.ru; Tel.: +7-921-953-0789

Abstract: Highly purified 5-vinyl-1*H*-tetrazole was synthesized, which is in great demand in modern medicine and industry as a monomer for obtaining nitrogen-rich macromolecular compounds and a reagent for the complete synthesis of biological compounds. The molecular structure was studied experimentally with sequential X-ray diffraction analysis and theoretically with ab initio quantum chemical calculations. The data from differential scanning calorimetry, nuclear magnetic resonance (¹H, ¹³C, ¹H-¹⁵N, HMBC), high-resolution mass spectrometry and vibrational spectroscopy were analyzed. The results are useful for evaluating the possibility of extending the polymerization of 5-vinyl-1*H*-tetrazole to synthesize polymers with predictable molecular weight and thermodynamic parameters.

Keywords: 5-vinyl-1*H*-tetrazole; synthesis; molecular structure; X-ray diffraction analysis; quantum chemical calculations; spectroscopy ¹H; ¹³C; ¹H-¹⁵N HMBC NMR; IR spectroscopy; mass spectrometry; differential scanning calorimetry



Citation: Krygina, D.M.; Sivtsov, E.V.; Pavlyukova, Y.N.; Chernova, E.N.; Skryl'nikova, M.A.; Baigildin, V.A.; Puzyk, A.M.; Oskorbyn, A.A.; Trifonov, R.E.; Aleshunin, P.A.; et al. 5-Vinyl-1*H*-tetrazole. *Molbank* **2023**, *2023*, M1565. <https://doi.org/10.3390/M1565>

Academic Editor: Rodrigo Abonia

Received: 22 December 2022

Revised: 16 January 2023

Accepted: 18 January 2023

Published: 23 January 2023



Copyright: © 2023 by the authors. Licensee MDPI, Basel, Switzerland. This article is an open access article distributed under the terms and conditions of the Creative Commons Attribution (CC BY) license (<https://creativecommons.org/licenses/by/4.0/>).

1. Introduction

Tetrazoles are the most nitrogen-rich azoles and are used as active ingredients in modern medicines, components of energy-saturated systems and functional materials [1,2]. It is notable that tetrazoles as well as 1,2,3-triazoles are the main objects of the Click-Chemistry and Bioorthogonal Chemistry concept of Carolyn R. Bertozzi, Morten Meldal and K. Barry Sharpless, who were awarded the Nobel Prize for Chemistry in 2022 [3].

A special member of this series of heterocyclic compounds is 5-vinyl-1*H*-tetrazole **1** and its N-alkyl derivatives, for example, compounds **2** and **3** (Figure 1) [4].

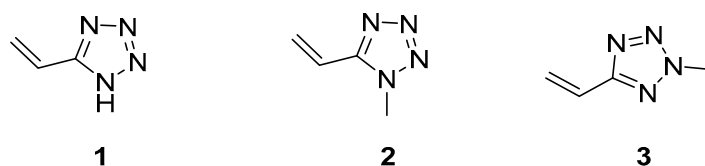


Figure 1. 5-vinyl-1*H*-tetrazole **1**, 1-methyl-5-vinyltetrazole **2**, 2-methyl-5-vinyltetrazole **3**.

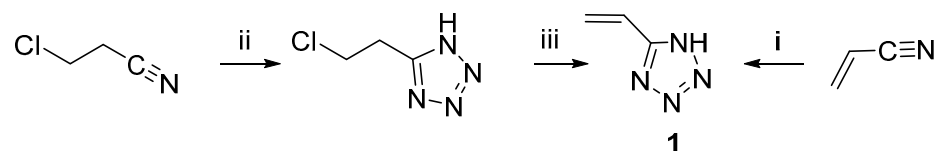
Due to the presence of the vinyl group in the molecular structure, which is activated by an electron-withdrawn tetrazole ring, compounds **1–3** can be used as monomers for obtaining nitrogen-rich high-molecular substances—poly-5-vinyltetrazoles. Possessing a unique set of physicochemical properties and operational characteristics, polyvinyltetrazoles are promising as a high-molecular basis for binding energy-intensive systems as well as medical materials [4,5]. Nowadays, these possibilities are disclosed only for N-substituted 5-vinyltetrazoles **2** and **3**, which have turned out to be interesting intermediate reagents for the complete synthesis of compounds with potential biological activity. In this context, recently, we have disclosed the Palladium-catalyzed Mizoroki-Heck cross-coupling reactions between N-methyl-5-vinyltetrazoles and aryl iodides in the presence of copper salts for the synthesis of 5-styryltetrazoles [6,7].

It is noteworthy that 5-vinyl-1*H*-tetrazole **1** is unique: in addition to the polarized C=C bond at the endocyclic carbon atom in the tetrazole ring, it has a “pyrrole” nitrogen atom—the NH group, capable of dissociation in accordance with the Brønsted–Lowry theory and forming H-bonded complexes with hydrogen-atom acceptors. This fact significantly expands the possibilities of 5-vinyltetrazoles’ functionalization, due not only to the reactivity of the C-vinyl group but also to reactions involving endocyclic nitrogen atoms of the tetrazole ring [8]. However, the known methods of synthesis are not suitable to obtain 5-vinyl-1*H*-tetrazole **1** with acceptable purification and good yields. The actual problem is to develop a rational synthesis method for tetrazole **1** and receive complete information about its molecular structure, stability, reactional properties and spectral properties.

2. Results and Discussion

2.1. Synthesis of 5-Vinyl-1*H*-tetrazole

First, 5-vinyltetrazole **1** was synthesized by Arnold C. and Thatcher D. from acrylonitrile or 5-chloroethyltetrazole according to Scheme 1 [9].

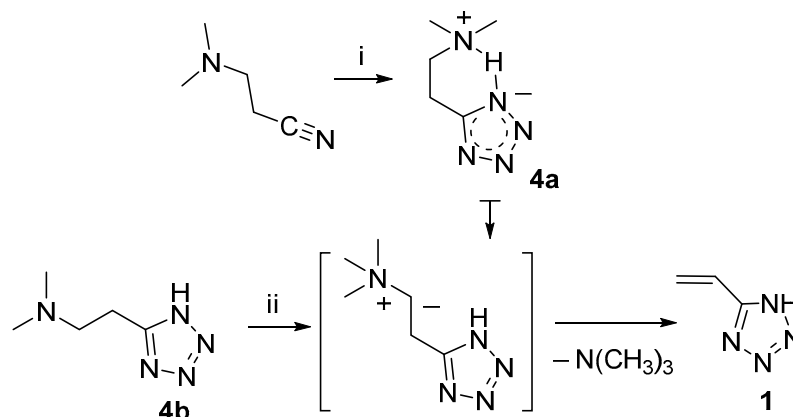


Scheme 1. The first synthesis of 5-vinyl-1*H*-tetrazole **1**. i, NaN_3 , AlCl_3 , N_2 , THF, reflux, 24 h, 15% HCl, mp (from CHCl_3 , charcoal) 126–127 °C, 55%; ii, NaN_3 , AlCl_3 , THF, N_2 , reflux 24 h, 15% HCl; iii, NaOH , H_2O , p-methoxyphenol, reflux, 2 h, mp (from CHCl_3 , charcoal) 126–127 °C, 70%.

The described methods did not spread widely in use: compound **1**, which was obtained under the conditions specified by the authors, is practically impossible to purify from polymer impurities [9]. Furthermore, aluminum oxide and hydrogen azide—byproducts in situ in the reaction mixture—are highly explosive and extremely toxic.

In this work, the synthesis of 5-vinyl-1*H*-tetrazole **1** was based on the two-stage method, which was published earlier by our scientific group [10]. In the first stage, as a result of 1,3-dipolar cycloaddition of dimethylammonium azide to β -dimethylaminopropionitrile in DMF, 5-(β -dimethylaminoethyl)tetrazole with a zwitter-ion structure **4a** was obtained, which precipitated [11]. In the second stage, exhaustive alkylation in H_2O of the terminal dimethylamino group of 5-(β -dimethylaminoethyl)tetrazole in normal form **4b** was carried out selectively, without affecting the tetrazole ring [10]. According to the mechanism established in work [12], trimethylammonium salt undergoes the elimination of trimethylamine with regeneration of the double bond (Hofmann elimination) in position 5 of the tetrazole ring, with the formation of 5-vinyl-1*H*-tetrazole (Scheme 2) [10]. This exact method is what we improve in the current work by introducing important minor adjustments for enhancing the quality of the product. As seen from Scheme 2 and following the synthesis method, we included an additional purification step for 5- β -dimethylaminoethyltetrazole with activated charcoal. Additionally, in the method used in [10], the obtained 5-vinyl-1*H*-tetrazole was dissolved in chloroform at the boiling point of the solvent (61.2 °C) before crystallization,

which often leads to the spontaneous polymerization of the product and increases its impurity. According to these circumstances, we dissolved 5-vinyl-1*H*-tetrazole **1** at a temperature not exceeding 50 °C before crystallization from chloroform.



Scheme 2. Synthesis of 5-vinyl-1*H*-tetrazole **1**. i, (CH₃)₂NN₃, DMF, 110 °C, 18 h, activated charcoal, mp 186 °C, 67%; ii, (CH₃O)₂SO₂, NaOH, H₂O (pH 14), 50–60 °C, 3.5 h, ionol, 0% HCl (pH 2), mp (from CH₃Cl, DSC-method), 131 °C, 55%.

2.2. Differential Scanning Calorimetry (DSC)

The thermal behavior of 5-vinyl-1*H*-tetrazole **1** was investigated using DSC. The melting point was determined to be 131.2 ± 0.5 °C (Figure 2). When the compound starts melting, a spontaneous polymerization occurs in the absence of any special initiator, obviously due to a thermal initiation. Under conditions of uncontrolled polymerization in the bulk of the monomer melt, the result is usually a cross-linked polymer that is insoluble in any solvent. At about 200 °C, polymerization finishes, and further heating leads to the degradation of poly(5-vinyltetrazole). The lower heating rate causes a narrower temperature range of melting and polymerization so that at the slow heating rate of 3 °C/min, the polymerization exotherm appears earlier than the melting endotherm.

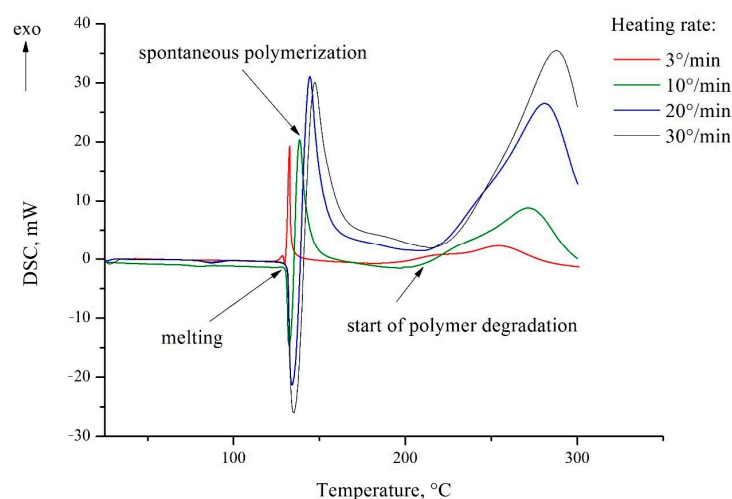


Figure 2. DSC thermograms of 5-vinyl-1*H*-tetrazole **1**.

2.3. X-ray Diffraction Analysis and Quantum Chemical Calculations

In the crystal (Figure 3), the molecules of 5-vinyl-1*H*-tetrazole **1** are held by a pair of NH⋯N hydrogen bonds, thus forming an infinite chain. In the lateral projection, these chains line up in almost flat plates. The distance between these plates varies and is about 3.2 Å.

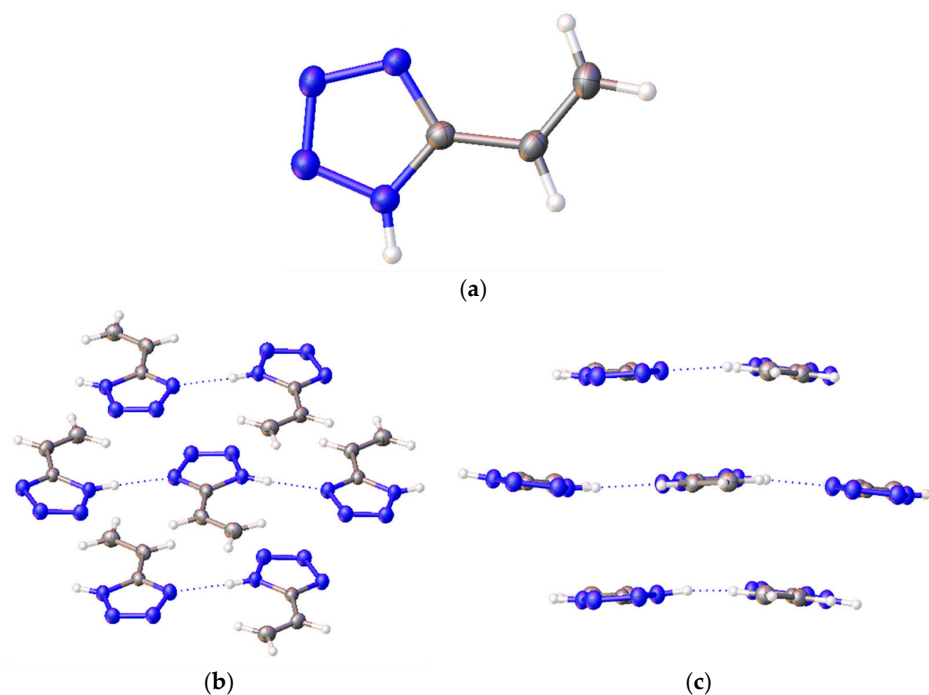


Figure 3. A structure of 5-vinyl-1H-tetrazole **1**: (a) one molecule; (b) frontal and (c) side view of a 5-vinyl-1H-tetrazole molecule chain.

The results of the X-ray diffraction of compound **1** are shown in Table 1. The crystals are monoclinic with dimensions of $0.1 \times 0.06 \times 0.03 \text{ mm}^3$.

Table 1. Crystal data and structure refinement parameters for 5-vinyl-1H-tetrazole **1**.

Crystal Data	Structure Refinement Parameters
CCDC number	2,226,676
Empirical formula	$\text{C}_3\text{H}_4\text{N}_4$
Molecular mass	96.10
Temperature, K	100(2)
Crystal system	monoclinic
Space group	$P2_1/c$
a, Å	7.7859(3)
b, Å	9.6724(3)
c, Å	6.7435(3)
α , °	90
β , °	115.262(5)
γ , °	90
Volume, Å ³	459.27(4)
Z	4
ρ_{calc} , g/cm ³	1.390
μ , mm ⁻¹	0.84
F (000)	200.0
Crystal size/mm ³	$0.1 \times 0.06 \times 0.03$
2 θ range for data collection/°	12.572 to 138.176
Index ranges	$-9 \leq h \leq 9, -11 \leq k \leq 11, -8 \leq l \leq 7$
Reflections collected	3211
Independent reflections	846 [$R_{\text{int}} = 0.0268, R_{\text{sigma}} = 0.0223$]
Data/restraints/parameters	846/0/73
Goodness-of-fit on F ²	1.049
Final R indices [$I \geq 2\sigma(I)$]	$R_1 = 0.0306, wR_2 = 0.0803$
Final R indices [all data]	$R_1 = 0.0318, wR_2 = 0.0812$
Largest diff. peak/hole/e Å ⁻³	0.23/−0.14

For theoretical calculations, the potential energy surface near the dihedral angle N4-C5-C6-C7 was scanned (the molecular model of vinyltetrazole with atomic numbering is shown in Figure 4). On a graph that describes the dependence of the potential energy of vinyltetrazole on the value of the dihedral angle N4-C5-C6-C7 (Figure 5), the energy of the most stable isomer was taken as zero, and the zero value of the dihedral angle corresponds to the structure of the molecule, as shown in Figure 4.

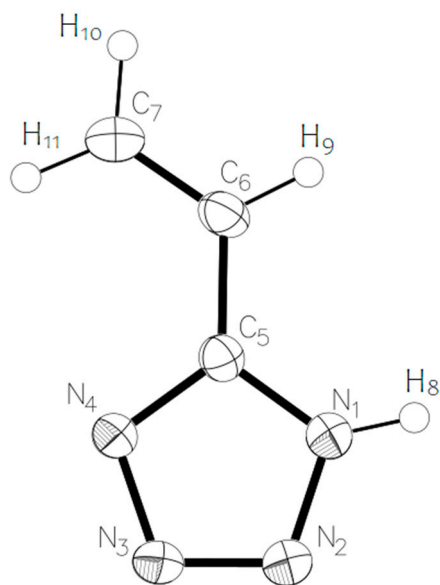


Figure 4. Molecular model of 5-vinyl-1*H*-tetrazole **1** with numbering of atoms.

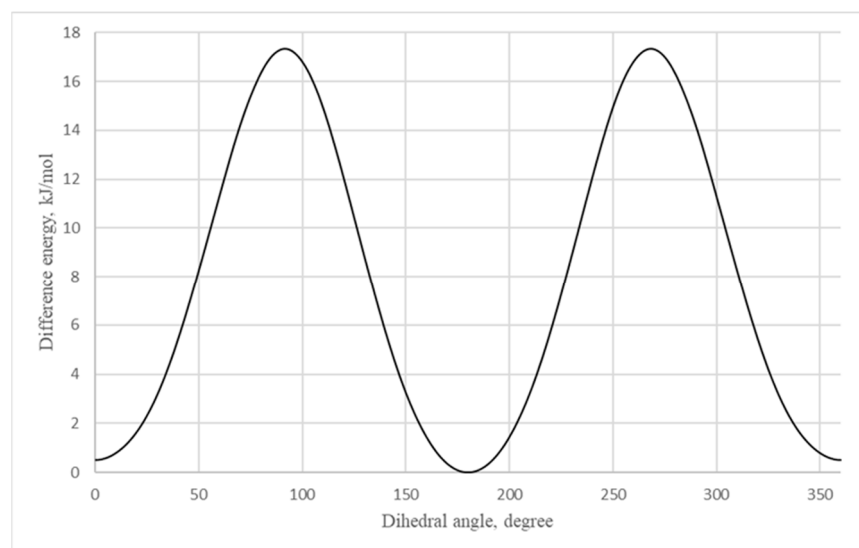


Figure 5. Dependence of the potential energy of 5-vinyl-1*H*-tetrazole **1** on the value of the dihedral angle N4-C5-C6-C7.

According to the calculation, the 1*H*-5-vinyltetrazole form has to be more stable in the gas phase with 0.5 kJ/mol more energy. The results of the X-ray diffraction show that a 4*H*- form of the molecule is prevalent in the crystal. This may be due to the presence of intramolecular cooperation: the occurring molecular energy of the 4*H*- form is greater than that of the 1*H*- form. However, it should be expected that there is a dynamic equilibrium between the two forms of the molecule's existence in a crystalline phase. The rotation barrier of the vinyl fragment is 17.3 kJ/mol.

The calculated quantum chemical and experimentally detected geometrical parameters of 5-vinyl-1*H*-tetrazole **1** are shown in Table 2 (with the numbering of atoms displayed in accordance with Figure 4).

Table 2. Calculated quantum chemical and experimentally detected geometrical parameters of 5-vinyl-1*H*-tetrazole **1**, rotational constants and dipole moment.

Parameter *	Experimental Values	B3LYP Calculation; Basis Set		
		6-311+G(d,p)	Three-Molecule System 6-311+G(d,p)	aug-cc-pVQZ
Bond lengths				
N1-N2	1.3534(14)	1.356	1.351	1.353
N2-N3	1.2932(15)	1.289	1.290	1.286
N3-N4	1.3527(13)	1.350	1.346	1.345
N1-C5	1.3314(14)	1.324	1.331	1.320
N4-C5	1.3300(14)	1.353	1.346	1.349
C5-C6	1.4547(15)	1.453	1.455	1.450
C6-C7	1.3225(17)	1.335	1.335	1.330
N4-H8	0.87(3)	1.008	1.034	1.005
C6-H9	0.950	1.084	1.086	1.081
C7-H10	0.950	1.083	1.083	1.079
C7-H11	0.950	1.085	1.085	1.082
Bond angles				
N1-N2-N3	108.46(9)	111.3	110.3	111.2
N2-N3-N4	108.14(9)	106.0	106.8	106.1
N2-N1-C5	107.93(9)	106.6	107.2	106.6
N3-N4-C5	108.19(9)	109.0	109.0	109.1
N1-C5-N4	107.3	107.1	106.7	107.1
N1-C5-C6	127.5	124.9	125.2	124.9
C5-C6-C7	123.63(11)	125.9	124.7	125.8
N3-N4-H8	120.4	119.9	118.5	120.0
C5-C6-H9	118.2	113.3	114.2	113.4
C6-C7-H10	120.0	120.8	120.3	120.9
C6-C7-H11	120.0	123.0	123.3	122.9
Rotational constants				
A	–	8727.04	–	8776.11
B	–	2095.33	–	2107.12
C	–	1689.65	–	1699.15
Dipole moment, μ	–	5.90	–	5.70

* Bond lengths in angstroms; angles in degrees; rotational constants in MHz; dipole moment in Debye.

The deviation between the calculated and experimental parameters is up to two-hundredths of an angstrom for the bond lengths and up to five degrees for the bond angles. Such a deviation may be connected with the fact that the calculations were performed for an isolated molecular system, whose geometrical parameters are fundamentally different from the parameters of a molecule in a crystal.

A topological analysis of the electron-density distribution in the three-molecule system was carried out (Figure 3c, in the middle). This type of analysis facilitates the recognition of critical bond points, which are defined as extrema of electron density. Critical points were assigned as p rank, equal to the number of non-zero eigenvalues of the Hess matrix, and as q rank, equal to the algebraic sum of the signs with non-zero eigenvalues. Thus, a set of four types of critical points was obtained: points (3; –3) correspond to the nucleus position, points (3; –1) are between chemically bonded atoms, points (3; +1) are inside a flat circle and (3;+3) are inside a three-dimensional closed structure. Such an analysis, among other things, reveals the presence of hydrogen bonds in organic compounds [13].

On the basis of the analysis results, a molecular graph using lines that connect critical points (3; –3) and (3; –1) was constructed (Figure 6). As is seen from the graph, between the hydrogen atoms of one molecule and the nitrogen atoms of another molecule, a critical

point of bond is observed. This means that a hydrogen bond exists in such a system, which corresponds with the results of the X-ray diffraction analysis. These critical point parameters and the characteristics of the nitrogen–hydrogen bond in the system with one molecule are presented in Table 3. The Laplacian electron density values $\nabla^2(\rho)$ show that the discussed intramolecular bonds have a different nature than the N–H covalent bonds with a Laplacian value of about -1.7 . A similar result is shown in the value of the electron density ρ , which is greater than 0.3 for covalently bonded atoms, while for the discussed hydrogen bonds it is 0.003 – 0.037 . The ellipticity parameter ε remains approximately the same for all the given bonds, but for the N2–(H–C) bond it sharply increases to 1.137 , which is most likely because of the interaction of the nitrogen atom with the pi electrons of the carbon–carbon double bond.

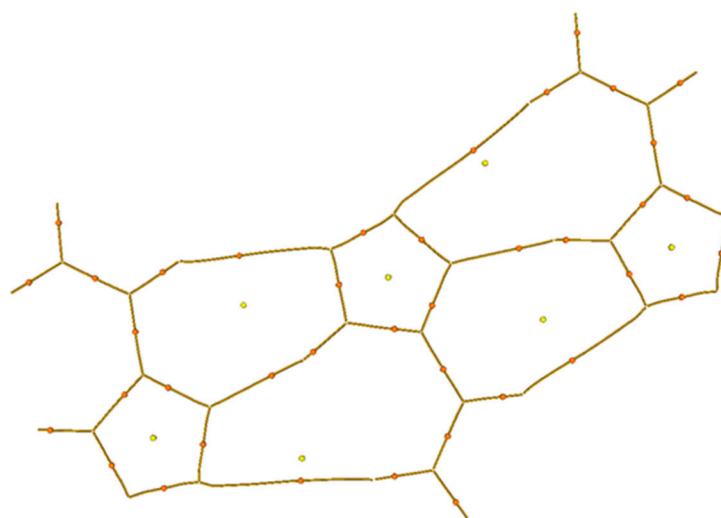


Figure 6. Molecular graph constructed using lines that connect critical points $(3; -1)$ and $(3; -3)$. Critical points of bond are denoted with orange color. Critical points of cycles are denoted with yellow color.

Table 3. Parameters of critical points of bonds in the one- and three-molecule system of 5-vinyl-1H-tetrazole 1.

Bond	$\nabla^2(\rho)$	ε	$\rho, \text{\AA}^{-3}$	H, a.u.
N4–H8 *	-1.771	0.042	0.340	-0.488
N4–H8	-1.730	0.033	0.314	-0.475
(N4–H8)–N **	0.097	0.060	0.037	-0.002
N1–(H–N) **	0.097	0.061	0.037	-0.002
N3–(H–C) **	0.018	0.050	0.006	0.001
N2–(H–C) **	0.009	1.137	0.003	0.000

* 1 molecule. ** value for hydrogen bond.

In general, the results of AIM analysis indicate the existence of hydrogen bonds. However, it is noteworthy that for N–(H–C) bonds, the density of the H energy has a positive value, which means that atom repulsion takes place in such an interaction. For this reason, these interactions are not hydrogen bonds, unlike bonds of the N–(H–N) type for which both the electron density is higher and the value of the energy density at the critical point is negative.

To describe the electron-density distribution, the charges of the atoms and the indices for the one- and three-molecule systems were calculated. The results are presented in Table 4. The calculations were made according to the theories of atoms in molecule (AIM) and natural bond orbitals (NBO). The table shows the charges of the atoms according to the definitions by Bader (AIM—charges) [14] and by Weinhold (NBO charges) [15]. The

bond order according to the Laplacian indices for AIM analysis and Wiberg bond indices for NBO analysis were used as bond-multiplicity indices.

Table 4. Calculated charges of atoms q and bond-multiplicity indices Q . For AIM, charges of atoms according to Bader and Laplacian bond order are presented. For NBO, NBO charges and Wiberg bond indices (WBI) are presented.

Parameter	AIM		NBO	
	1 mol	3 mol	1 mol	3 mol
$q(\text{N1})$	−0.600	−0.663	−0.296	−0.373
$q(\text{N2})$	−0.057	−0.076	−0.066	−0.066
$q(\text{N3})$	−0.069	−0.092	−0.064	−0.082
$q(\text{N4})$	−0.763	−0.789	−0.363	−0.374
$q(\text{C5})$	0.910	0.913	0.308	0.347
$q(\text{C6})$	0.016	0.008	−0.233	−0.258
$q(\text{C7})$	−0.019	−0.018	−0.322	−0.298
$q(\text{H8})$	0.442	0.516	0.420	0.456
$q(\text{H9})$	0.073	0.101	0.232	0.248
$q(\text{H10})$	0.051	0.054	0.206	0.205
$q(\text{H11})$	0.016	0.046	0.179	0.193
$Q(\text{N1-N2})$	0.845	0.848	1.320	1.316
$Q(\text{N2-N3})$	1.236	1.217	1.615	1.595
$Q(\text{N3-N4})$	0.806	0.832	1.218	1.239
$Q(\text{N4-C5})$	1.008	0.590	1.212	1.251
$Q(\text{N1-C5})$	1.308	1.245	1.490	1.436
$Q(\text{C5-C6})$	1.204	1.189	1.091	1.092
$Q(\text{C6-C7})$	1.761	1.757	1.905	1.900
$Q(\text{N4-H8})$	0.689	0.590	0.793	0.692
$Q(\text{C6-H9})$	0.834	0.832	0.904	0.893
$Q(\text{C7-H10})$	0.847	0.849	0.937	0.937
$Q(\text{C7-H11})$	0.841	0.845	0.944	0.938
$Q(\text{N1-H-N})$	0.0001		0.072	
$Q(\text{N4-H8-N})$	0.0001		0.072	

The NBO charges of the atoms are represented for one molecule (Figure 7a) and for a system of three molecules (Figure 7b).

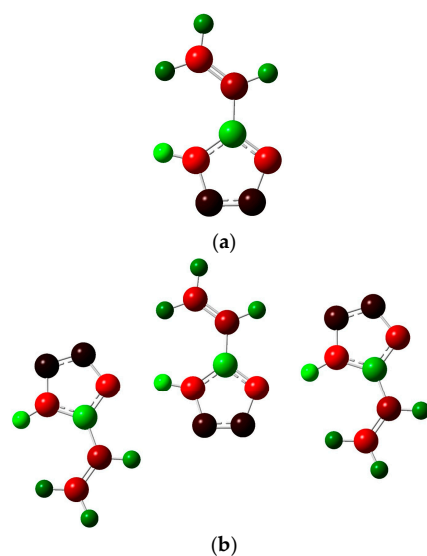


Figure 7. Distribution of NBO atom charges in one 5-vinyl-1H-tetrazole molecule (a) and in a system of three molecules; (b) green-colored atoms have a positive charge, red-colored atoms have a negative charge and black-colored atoms have zero charge.

On the whole, the nature of a charge distribution corresponds to general chemical concepts. It could be noticed that the N4-H8 bond in the three-molecule system weakens compared to the single molecule, which is associated with hydrogen bond formation. The Laplacian bond order for such hydrogen bonds is about 10^{-4} , while the Wiberg bond index for them is about 0.07. This indicates the low energy of such interactions, which is consistent with the characteristics of the critical points given above.

To provide a description of the electron-density distribution and chemical properties of 5-vinyl-1*H*-tetrazole, the energy levels of the highest occupied molecular orbital (HOMO) and lowest unoccupied molecular orbital (LUMO) were calculated (Figure 8). The energies of these orbitals correspond with the ability to donate and accept electrons, respectively.

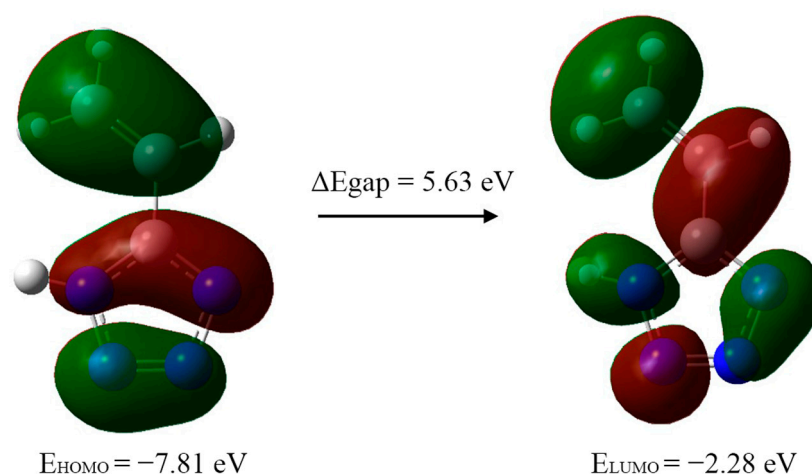


Figure 8. Computed energy levels HOMO–LUMO of 5-vinyl-1*H*-tetrazole **1** in gas phase.

On the basis of the HOMO and LUMO energies, the reactivity indices were calculated: ionization potential ($IP = -E_{HOMO}$), electron affinity ($EA = -E_{LUMO}$), electrophilicity index ($\omega = \mu^2/2\eta$), chemical potential ($\mu = -(IP + EA)/2$), electronegativity ($\chi = (IP + EA)/2$) and hardness ($\eta = IP - EA$) (Table 5). The calculation was performed on the basis of Koopmans' theorem, which shows that the HOMO and LUMO energies are practically equal to the ionization potential and electron affinity, respectively. The energy difference between HOMO and LUMO, the so-called energy gap, is an indicator of the stability and reactivity of the compound [16] and is used for the description of organic compound reactivity [17]. In this case, its value indicates the stability of the synthesized 5-vinyl-1*H*-tetrazole.

Table 5. HOMO and LUMO orbital energies (eV) and global reactivity descriptors (eV) of 5-vinyl-1*H*-tetrazole **1**.

Parameter	Value
HOMO energy	−7.81
LUMO energy	−2.18
HOMO–LUMO energy gap	5.63
Ionization potential (IP)	7.81
Electron affinity (EA)	2.18
Electrophilicity index (ω)	4.43
Chemical potential (μ)	−4.99
Electronegativity (χ)	4.99
Hardness (η)	5.63

To describe the reactivity, we also calculated the values of the Fukui functions f^+ [16], which are equal to the difference in electron density at a given point between the system with $N + 1$ number of electrons and the initial system with N number of electrons. A visualization of the obtained results is shown in Figure 9. Areas with a positive Fukui

function value are green-colored, and areas with a negative Fukui function value are blue-colored. Thus, in the green areas, an additional electron is predominantly distributed. A nucleophilic attack will predominantly occur in the same areas because a nucleophile is an electron-rich system.

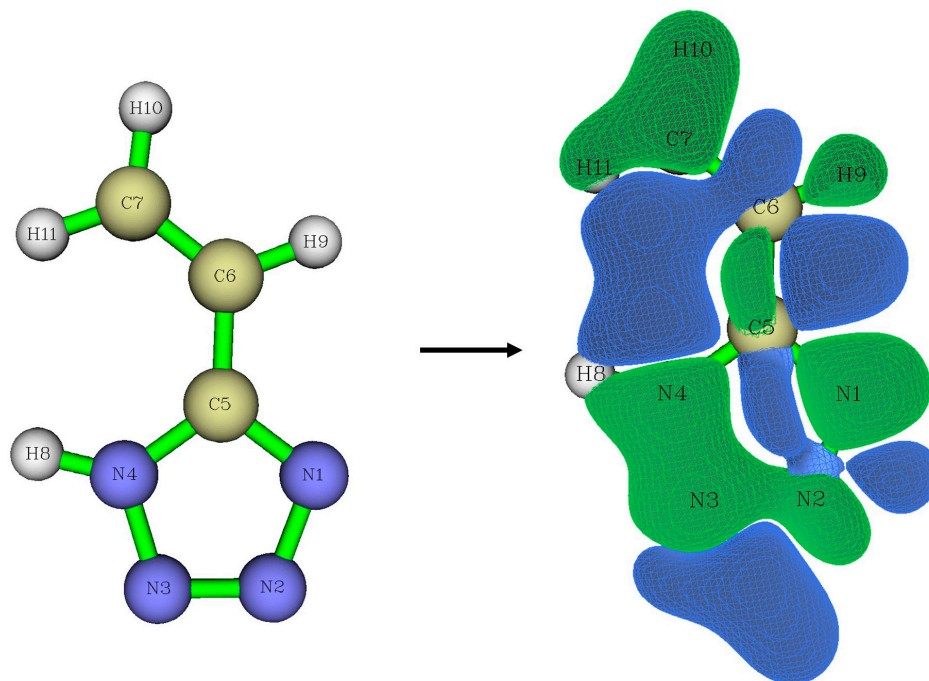


Figure 9. Visualization of Fukui functions f_+ .

2.4. Infrared Spectroscopy

The IR spectra of the one-molecule system (Figure 10) and three-molecule system (Figure S1 in Supplementary Materials) were obtained, analyzed and interpreted.

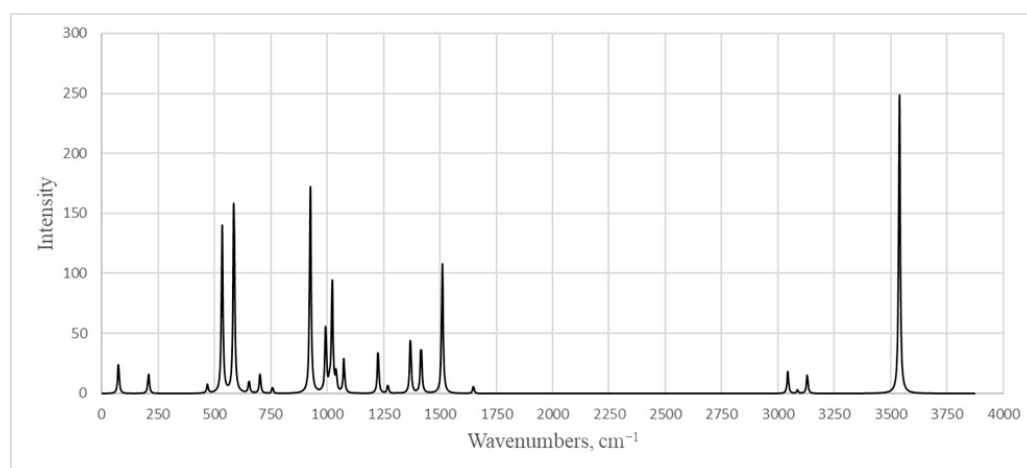


Figure 10. Calculated infrared spectrum of 5-vinyl-1H-tetrazole 1.

It is worth noting that the signal of an intense band corresponding to vibrations of the N–H bond at 3500 cm^{-1} is absent (Figures S2 and S3). Taking this into account, those spectra were inferred to be the crystals of 5-vinyl-1H-tetrazole 1. Analyzing the results of the X-ray diffraction analysis and quantum chemical calculations, we can assume that the reason is the presence of the proton of the cycle in the composition of the linear associates $\text{–N-1–H}\cdots\text{N-4–}$, where nitrogen atoms belong to the cycles of neighboring molecules. This fact

was highlighted earlier as the characteristic feature of the crystals of all NH-unsubstituted tetrazoles [18]. Then, the vibration of the proton is consistent; for example, the stretching of the N-1–H bond is accompanied by the contraction of the H···N-4 bond and vice versa. This is accompanied by a shift in the resonant frequency to the lower wave number area. Interestingly, in the IR spectrum of the N-vinyl pyrrolidone and 5-vinyl-1H-tetrazole **1** copolymer sample, which contained only 5 mol% of 5-vinyltetrazole units, a band appeared at 3500 cm⁻¹ (Figure S4). Because the spectrum of N-vinylpyrrolidone has no absorption in this region (Figure S5), a band corresponds to the calculated related vibrations of the N–H bond. The difference between the polymer and monomer crystals is that the tetrazole rings were linked to the polymer chain and depended on its molecular dynamics. This makes it impossible to form associates similar to those found in the crystals of the 5-vinyl-1H-tetrazole **1** itself.

The above reasoning is confirmed by the results of quantum chemical calculations. In the calculated IR spectrum for the three-molecule system, there are 2 peaks: 3531 cm⁻¹ corresponds to stretching vibrations of the N-H side molecule, and 3075 cm⁻¹ (the intense band) corresponds to stretching vibrations of H atoms bound by hydrogen bonds. Apparently, a corresponding vibration occurs in the experimental spectrum at the peaks of 3116 cm⁻¹ (Figure S2) and 3114 cm⁻¹ (Figure S3). A large difference between the experimental and calculated intensity of the discussed peaks is explained by the fact that for the vibrations that appear in the IR spectrum, the intensity is proportional to the change in the dipole moment for a given vibration. At the same time, with the scaling of a system's size (in this case, an increase in the number of links in the chain), the dipole moment stabilizes and depends less and less on the vibration of the atom, which leads to a decrease in the vibrations' intensity. Vibrations were observed in both the experimental and theoretical spectra (theoretical value is given in parentheses): 674.1 (653.3) cm⁻¹ corresponds to deformation vibrations of the vinyl fragment; 781.2 (757.5) cm⁻¹ corresponds to torsional vibrations of both the vinyl fragment and the ring; 935.5 (925.4) cm⁻¹ corresponds to torsional vibrations of CH₂; 962.5 (975.4) cm⁻¹ corresponds to bending vibrations of the ring; 1050.3–1248.0 cm⁻¹ peaks refer to stretching vibrations of the tetrazole ring; the 1371.45 (1369.2) and 1559.51 (1510.5) cm⁻¹ peaks correspond to deformation symmetric CH-CH₂ vibrations (in this case, the second peak corresponds to a vibration with a large amplitude of the endocyclic carbon atom); the 1645.3 (1648.3) cm⁻¹ peak corresponds to stretching vibrations of the vinyl fragment; and the 2872.13 (3042.3), 2924.2 (3085.3) and 2998.5 (3128.4) cm⁻¹ peaks refer to stretching vibrations of hydrogen atoms in the vinyl fragment. It should be noted that we used a scaling multiplier of 0.9688 for the entire range of wave numbers, and in the region of the small wave numbers, the theoretical values are somewhat underestimated compared to the experimental ones. Peaks at about 1000–1300 cm⁻¹ converge well, and peaks in the region above 2000 cm⁻¹ are strongly overestimated. Peaks that are not indicated above and that are absent from both the calculated spectra for the system of one molecule and for the system of three molecules (in the region of 2200–2850 cm⁻¹) were most likely interplanar vibrations in the vinyltetrazole crystal.

2.5. Mass Spectrometry

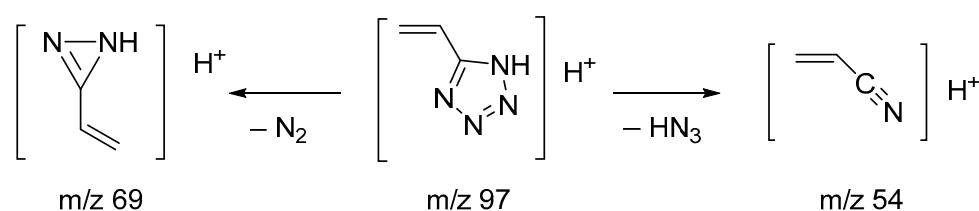
In order to confirm the structure of the synthesized compound and study the pathways of mass spectrometric fragmentation, high-resolution mass spectra in full-scan mode and tandem spectra for the protonated molecular ion were obtained. In the spectra recorded using electrospray mass spectroscopy (ESI-MS) in positive mode, a molecular ion with *m/z* 97.05087 was detected. Its mass differed from the theoretical (calculated) mass of 5-vinyl-tetrazole by 0.23 ppm, which fit into the mass measurement accuracy criterion (5 ppm) when identifying compounds using an LTQ Orbitrap high-resolution mass spectrometer.

The fragmentation of the molecular ions of the studied substance was strongly influenced by the collision energy in the fragmentation cell. Thus, with an increase in the fragmentation energy, the intensity of the molecular ion signal noticeably decreased [M+H]⁺ (*m/z* = 97), and the intensity of the fragment ions increased (*m/z* = 54) (Table 6).

Table 6. Product ions formed from the precursor ion of m/z 97 ($[M+H]^+$) and their intensities in tandem mass spectra acquired at three different collision energy levels.

Collision Energy, %	Product Ions	Absolute Intensity	Relative Intensity, %
10	97	2590	100
20	54	170	10
	97	1680	100
35	54	850	100
	69	10	1

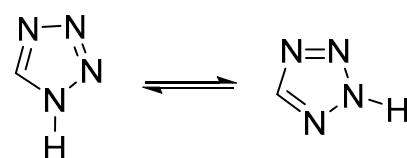
The mass spectral fragmentation of 5-vinyl-1H-tetrazole mainly proceeded with the elimination of HN_3 (product ion with m/z 54), which was also noted by Forkey and Carpenter when studying the fragmentation of tetrazole, 5-methyltetrazole and 1,5-dimethyltetrazole [19]. At high ionization energies, the nitrogen molecule (product ion with m/z 69) was eliminated, which is characteristic of all tetrazole derivatives [19] (Scheme 3).

**Scheme 3.** Proposed fragmentation pathways for 5-vinyl-1H-tetrazole 1.

2.6. NMR Spectroscopy

A group of signals of protons in the vinyl group, a proton cycle in a very weak field and three signals of carbon atoms are expected to be observed in the NMR ^1H and ^{13}C spectra. The endocyclic carbon atom is visible in the weakest field (Figures S6 and S7).

Tetrazole has only two existing tautomeric forms from the four possible tautomers: 1H-tetrazole and 2H-tetrazole (Figure 11). The 1H-tautomer predominates in the condensed phase and polar solvents, whereas 2H-tetrazole is more stable in the gas phase [20].

**Figure 11.** 1H- and 2H- tautomeric forms of the tetrazole.

It should be noted that virtually all NH-unsubstituted 5-substituted tetrazoles, regardless of the substituent, exist in the crystalline state as individual 1H-tautomers [1,18].

According to the data of the 2D correlation spectrum ^1H - ^{15}N HMBC, the proton of the CH group, which is in the alpha position to the tetrazole ring, has two significant cross-peaks with two types of nitrogen atoms at 177.7 and 345.7 ppm, while the protons of the CH_2 group have cross-peaks with only one nitrogen atom at 177.4 ppm (Table 7, Figure S8). Obviously, such a picture can be observed because of the fast intermolecular exchange of protons between the nitrogen atoms in positions 1 and 4 of the heteroring, which leads to an averaging of the characteristics of the N^1 and N^4 atoms as well as N^2 and N^3 . Similar effects were noted previously [20]. The probability of tautomeric transformations of 1H/2H-tetrazole seems unlikely under these conditions [18].

Table 7. Cross-peaks in ^1H - ^{15}N HMBC spectrum of 5-vinyl-1*H*-tetrazole **1**.

^1H	Cross-Peaks
H-9 (6.83ppm)	−43.5 (weak); −32.3; −21.7; 87.7; 177.7; 345.7; 353.2 (weak); 409.5 (weak); 415.7; 434.9
H-11 (6.25 ppm)	132.7; 133.3; 177.4 (strong); 346.2; 353.1 (strong)
H-10 (5.81 ppm)	178.5 (strong); 299.1 (strong); 408.8 (strong)

3. Materials and Methods

3.1. Synthesis of 5-Vinyl-1*H*-tetrazole **1**

5-(β -dimethylaminoethyl)tetrazole **4** was synthesized according to the following procedure. 12.6 g (154 mmol) of dimethylamine hydrochloride was dissolved in 70 mL of DMF, then 10 g (154 mmol) of sodium azide was added in portions to the obtained solution. The reaction mixture was stirred for 2 h at 40–50 °C. After cooling to room temperature, a solution of dimethylammonium azide was filtered from sodium chloride and used at the next stage in dissolved form. Then, 15.1 mL (134 mmol) of β -dimethylaminopropionitrile was added to a solution of dimethylammonium azide. The reaction mixture was stirred for 18 h at 110 °C. After exposure, the reaction mixture was first cooled to room temperature, then to 0 °C. The reaction product was filtered off under vacuum and washed with acetone (3 \times 20 mL). For the purification, 5-(β -dimethylaminoethyl)tetrazole **4** was dissolved in 100 mL of distilled water, and approximately 1 g of finely dispersed activated charcoal was added. Exposure lasted until the complete discoloration of the solution. The purified product was filtered from charcoal and drained from water in vacuum. The yield was 12.7 g (67%) of colorless crystals.

Further, 10 g (70 mmol) of 5-(β -dimethylaminoethyl)tetrazole **4** was dissolved in 35 mL of distilled water. Then, 5.7 g (141 mmol) of sodium hydroxide was dissolved in 35 g of ice to avoid heating and was added in portions. The resulting solution (pH~14) was stirred for 15 min at room temperature. Then, 9.9 g (78 mmol) of freshly distilled dimethyl sulfate was added dropwise. The reaction mixture was heated at 50 °C and stirred for 3.5 h. After exposure, the reaction mixture was cooled to 5 °C. To avoid spontaneous polymerization of 5-vinyl-1*H*-tetrazole, an inhibitor was added: several crystals of hydroquinone or ionol. Then, concentrated hydrochloric acid was added dropwise until the pH value reached 2. The reaction mixture was extracted with ethyl acetate (7 \times 30 mL), and the combined extract was dried with anhydrous Mg_2SO_4 for 12 h. The drying agent was removed with filtration, and the solvent was removed in vacuum. The purification by crystallization was carried out. 5-vinyl-1*H*-tetrazole **1** was added to 30 mL of chloroform and heated slowly at 50 °C until the substance had completely dissolved. Next, hot filtration was carried out. The obtained colorless crystals were filtered under vacuum and dried. The yield was 3.7 g (55%). The melting point was 131 °C (DSC-method).

^1H NMR spectrum (400 MHz, DMSO- d_6) δ , ppm: 16.00. (s, 1H), 6.86–6.80 (dd, J = 17.8, 11.3 Hz, **H-9**, CH), 6.24–6.27 (dd, J = 17.8, 0.9 Hz, **H-11**, CH_2), 5.80–5.83 (dd, J = 11.3, 0.9 Hz, **H-10**, CH_2). ^{13}C NMR spectrum (126 MHz, DMSO- d_6) δ , ppm: 154.10, 125.16, 120.37.

3.2. Synthesis of Copolymer of *N*-Vinylpyrrolidone with 5-Vinyl-1*H*-tetrazole

The block copolymer p(*N*-vinylpyrrolidone-*b*-vinyltetrazole) was synthesized using reversible addition–fragmentation chain-transfer polymerization (RAFT). p(*N*-vinylpyrrolidone) based on a RAFT agent, *S*-benzyl *O*-ethylcarbonodithioate, was applied as a macro-RAFT agent with an average molecular weight of 4100 and a polydispersity of 1.11. Typically, the macro-RAFT agent 95 mol.%, azobisisobutyronitrile as an initiator (10^{-3} M) and 5-vinyl-1*H*-tetrazole (5 mol.%) were added to dioxane (10 mL) and placed in a Pyrex reactor, degassed with three repeated freeze–evacuate–thaw cycles and sealed. The polymerization was carried out at 70 °C for 6 h. The obtained block copolymer was purified through re-precipitation from diethyl ether and chloroform. The yield equaled ca. 85%.

3.3. Materials and Equipment

3.3.1. Characteristics of the Quantum Chemical Method, Baselines

The theoretical calculations were performed with the GAUSSIAN09 [21] program package using a Becke-style [22] three-parameter density functional with a Lee–Yang–Parr correlation functional B3LYP [23] and the 6-311+G(d, p) basis set that contains diffuse and polarization functions. In addition, calculations were performed with the aug-cc-pVQZ basis set that contains four basis functions for each valence orbital, diffuse and polarizations functions and additional basis functions to account for electron correlation.

Frequency calculations and an electron structure analysis were performed on the B3LYP/6-311+G(d,p) level of theory with the Multiwfn [24] and NBO 3.1 programs.

The calculated harmonic wavenumbers were scaled down using a single scale factor of 0.9688 [25].

3.3.2. Mass Spectrometry

The target compound was identified using high-performance liquid chromatography–high-resolution mass spectrometry (HPLC-MS-HR) using a Prominence LC-20 HPLC system (Shimadzu, Duisburg, Germany) in combination with an LTQ Orbitrap XL mass spectrometer (Thermo Fisher Scientific, San Jose, CA, USA). A Luna Omega C18 reverse phase column (100 × 2.1 mm, 3 μm, Phenomenex) was used in the gradient elution mode (content of the organic component from 40 to 90%) at a flow rate of 0.3 mL/min with a mixture of water and acetonitrile. Mass spectrometric analysis was performed under electrospray ionization conditions in the positive ion detection mode. The ion mass scanning range was m/z 70–200. The target compound was identified on the basis of accurate ion mass measurements with a resolution of 30,000 and an accuracy within 5 ppm. Fragment spectra were obtained in a linear ion trap by varying the collision energy (10%, 20%, 35%) in the CID mode (Collision Initiated Dissociation).

3.3.3. Differential Scanning Calorimetry (DSC)

Differential scanning calorimetry (DSC) was performed using a Shimadzu DSC-60 Plus differential scanning calorimeter (Kyoto, Japan). The analysis was carried out in a N₂ atmosphere (flow rate 100 mL/min) with samples of approximately 2.8 mg at a scanning speed of 3, 10, 20 and 30 °C/min in the temperature range from 273 K to 573 K. Data processing was carried out using ShimadzuCorporation@ta60 Version 2.21.

3.3.4. X-Ray Diffraction Analysis

Single crystal X-ray diffraction measurements were conducted with a SuperNova, Single source at offset/far, HyPix3000 diffractometer. The crystal was kept at 100 K during data collection. The structures were solved with the SHELXT program [26], using least-squares minimization in an anisotropic (for non-hydrogen atoms) approximation and refined with the SHELXL [27] package incorporated in the Olex2 [28] program package. The hydrogen atoms were introduced to the geometrically calculated positions and refined by attaching themselves to the corresponding parent atoms. Empirical absorption correction was applied in the CrysAlisPro (Rikagu Oxford Diffraction; CrysAlisPro; Agilent Technologies Inc.: Yarnton, Oxfordshire, UK, 2018) program complex using spherical harmonics and implemented in SCALE3 ABSPACK scaling algorithm.

The supplementary crystallographic data for this paper have been deposited at the Cambridge Crystallographic Data Centre (CCDC 2226676) and can be obtained free of charge via www.ccdc.cam.ac.uk/data_request/cif.

3.3.5. NMR Spectroscopy

The solution ¹H, ¹³C{¹H} NMR spectra were recorded on a Bruker Avance III 400 MHz spectrometer in DMSO-d₆. The solution ¹H-¹⁵N HMBC NMR spectra were recorded on a Bruker Avance III 500 MHz. The reference used for the 2D spectra was ammonium nitrate.

3.3.6. IR Spectroscopy

Spectra were registered using an Infrared Fourier spectrometer Shimadzu IRAffinity-1 in KBr and attenuated total reflectance (ATR) accessory, model Quest Single Reflection (SPECAC).

4. Conclusions

The results of a comprehensive study of the molecular structure and spectral properties of 5-vinyl-1*H*-tetrazole **1** have been described. Compound **1** is an indispensable monomer for receiving a nitrogen-rich high-molecular base in the new-generation functional materials that are in demand in modern medicine and technology. Using previously known methods of synthesis, it is impossible to obtain pure vinyltetrazole **1**. Furthermore, impurities catalyze uncontrolled polymerization and occur both in the crystalline phase (in bulk) and in solutions. We solved this problem in the framework of this study and synthesized a stable 5-vinyl-1*H*-tetrazole **1** that is not polymerized spontaneously. Improvements in compound **1** quality made it possible to establish the details of its molecular structure using X-ray crystallography, differential scanning calorimetry (DSC), nuclear magnetic resonance (^1H , ^{13}C , ^1H - ^{15}N , HMBC NMR), high-resolution mass spectrometry (HRMS) and vibrational spectroscopy. In addition, we used *ab initio* quantum chemical calculations, which are helpful for a comprehensive interpretation of the experimental data. The results enable us to apply fundamentally new methods for the controlled polymerization of tetrazole structures (for example, RAFT polymerization) and to obtain polymers with a complex architecture and specified physicochemical characteristics.

Supplementary Materials: The following supporting information can be downloaded online. Figure S1: Calculated infrared spectrum for the three 5-vinyl-1*H*-tetrazole molecule system; Figure S2: IR spectrum of 5-vinyl-1*H*-tetrazole (in KBr); Figure S3: IR spectrum of 5-vinyl-1*H*-tetrazole (obtained using attenuated total reflectance (ATR) accessory); Figure S4: IR spectrum of copolymers synthesized from monomer mixture N-vinyl pyrrolidone/5-vinyl-1*H*-tetrazole =95/5 (mol.%); Figure S5: IR spectrum of N-vinyl pyrrolidone; Figure S6: ^1H NMR spectrum of 5-vinyl-1*H*-tetrazole in DMSO- d_6 ; Figure S7: ^{13}C NMR spectrum of 5-vinyl-1*H*-tetrazole in DMSO- d_6 ; Figure S8: ^1H - ^{15}N HMBC NMR spectrum of 5-vinyl-1*H*-tetrazole in DMSO- d_6 .

Author Contributions: Conceptualization, E.V.S. and V.A.O.; methodology, P.A.A. and V.A.O.; formal analysis, E.V.S., A.M.P., E.N.C., A.A.O. and R.E.T.; investigation, D.M.K., E.V.S., E.N.C., V.A.B., A.M.P., A.A.O., R.E.T. and V.A.O.; resources, D.M.K., E.V.S., E.N.C., V.A.B., A.M.P. and A.A.O.; data curation, E.V.S. and V.A.O.; writing—original draft preparation, E.V.S., V.A.O., D.M.K., E.N.C., A.A.O. and Y.N.P.; writing—review and editing, M.A.S. and D.M.K.; project administration, E.V.S. and V.A.O. All authors have read and agreed to the published version of the manuscript.

Funding: This research was funded by the Russian Foundation for Basic Research and the Committee on Science of the Republic of Armenia within the framework of the scientific project No. 20-53-05010 Arm_a/20RF-138 and by the grant program for young scientists FASIE (2022–2023) No. 17837GU/2022. The work of the author from IMC RAS was supported by the Ministry of Science and Higher Education of the Russian Federation as part of the State Assignment of IMC RAS (project no. AAAA-A20-120022090039-8).

Institutional Review Board Statement: Not applicable.

Informed Consent Statement: Not applicable.

Acknowledgments: The authors are grateful to the Engineering Center of the St. Petersburg State Technological Institute, Technical University, and the Research Park of St. Petersburg State University for the technical support. This study was carried out using the equipment of the Research Park of St. Petersburg State University Centers for Magnetic Resonance and for Chemical Analysis and Materials Research.

Conflicts of Interest: The authors declare no conflict of interest.

Sample Availability: Samples of the compounds are not available from the authors.

References

1. Ostrovskii, V.A.; Popova, E.A.; Trifonov, R.E. Tetrazoles. In *Comprehensive Heterocyclic Chemistry IV*; Black, D., Cossy, J., Stevens, C., Eds.; Elsevier: Oxford, UK, 2022; Volume 6, pp. 182–232. [[CrossRef](#)]
2. Pasquinet, E. Nitrogen-Rich Polymers as Candidates for Energetic Applications. In *New Polymers for Special Applications*; De Souza Gomes, A., Ed.; IntechOpen: London, UK, 2012. [[CrossRef](#)]
3. Demko, Z.P.; Sharpless, K.B. Preparation of 5-Substitution 1*H*-tetrazoles from nitriles. *J. Org. Chem.* **2001**, *66*, 7945–7950. [[CrossRef](#)] [[PubMed](#)]
4. Kizhnyaev, V.N.; Vereshchagin, L.I. Vinyltetrazoles: Synthesis and properties. *Russ. Chem. Rev.* **2003**, *73*, 143–164. [[CrossRef](#)]
5. Ostrovskii, V.A.; Pevzner, M.S.; Kofman, T.P.; Shcherbinin, M.B.; Tselinskii, I.V. Energetic 1,2,4-Triazoles and Tetrazoles: Synthesis, Structures and Properties. In *Targets in Heterocyclic Systems: Chemistry and Properties*; Attanasi, O.A., Spinelli, D., Eds.; Italian Society of Chemistry: Roma, Italy, 1999; Volume 1, pp. 467–526.
6. Aleshunin, P.A.; Esikov, K.A.; Dolgushin, F.M.; Ostrovskii, V.A. Vinyltetrazoles: III. Metal-catalyzed arylation, a new method of vinyltetrazoles functionalization. *Russ. J. Org. Chem.* **2012**, *48*, 1464–1472. [[CrossRef](#)]
7. Lisakova, A.D.; Ryabukhin, D.S.; Trifonov, R.E.; Ostrovskii, V.A.; Vasilyev, A.V. Heck reaction of 2-methyl-5-vinyl-2*H*-tetrazole with iodoarenes. *Russ. J. Org. Chem.* **2015**, *51*, 290–291. [[CrossRef](#)]
8. Pavlyukova, Y.N.; Trifonov, R.E.; Yugai, E.V.; Aleshunin, P.A.; Tselinskii, I.V.; Ostrovskii, V.A. Kinetics and mechanism of 5-vinyltetrazole alkylation. *Russ. J. Org. Chem.* **2008**, *44*, 1711–1715. [[CrossRef](#)]
9. Arnold, C., Jr.; Thatcher, D.N. Preparation and reactions of 5-vinyltetrazole. *J. Org. Chem.* **1969**, *34*, 1141–1142. [[CrossRef](#)]
10. Ostrovskii, V.A.; Aleshunin, P.A.; Zubarev, V.Y.; Popova, E.A.; Pavlyukova, Y.N.; Shumilova, E.A.; Trifonov, R.E.; Artamonova, T.V. Vinyltetrazoles: I. Synthesis of NH-unsubstituted 5-vinyltetrazole. *Russ. J. Org. Chem.* **2010**, *46*, 1678–1681. [[CrossRef](#)]
11. Ostrovskii, V.A.; Poplavskii, V.S.; Shcherbinin, M.B. Acid-base properties and the structure of the 5-(2-dimethylaminoethyl)tetrazole. *Russ. J. Org. Chem.* **1998**, *34*, 870–875.
12. Ostrovskii, V.A.; Podkameneva, M.E.; Poplavskii, V.S.; Trifonov, R.E. Kinetics and mechanism of formation of isomeric 1-methyl and 2-methyl-5-vinyltetrazoles. *Russ. Chem. Bull.* **2009**, *58*, 2147–2153. [[CrossRef](#)]
13. Espinosa, E.; Molins, E.; Lecomte, C. Hydrogen bond strengths revealed by topological analyses of experimentally observed electron densities. *Chem. Phys. Lett.* **1998**, *285*, 170–173. [[CrossRef](#)]
14. Bader, R.F.W. *Atoms in Molecules: A Quantum Theory*; Oxford University Press: New York, NY, USA, 1994; 456p.
15. Glendening, E.D.; Landis, C.R.; Weinhold, F. Natural bond orbital methods. *Wiley Interdiscip. Rev. Comput. Mol. Sci.* **2012**, *2*, 1–42. [[CrossRef](#)]
16. Fukui, K. Theory of orientation and stereoselection. In *Orientation and Stereoselection*; Springer: Berlin/Heidelberg, Germany, 1970; pp. 1–85.
17. Nataraj, A.; Balachandran, V.; Karthick, T. Molecular orbital studies (hardness, chemical potential, electrophilicity, and first electron excitation), vibrational investigation and theoretical NBO analysis of 2-hydroxy-5-bromobenzaldehyde by density functional method. *J. Mol. Struct.* **2013**, *1031*, 221–233. [[CrossRef](#)]
18. Ostrovskii, V.A.; Koldobskii, G.I.; Trifonov, R.E. Tetrazoles. In *Comprehensive Heterocyclic Chemistry III*; Katritzky, A.R., Ramsden, C.A., Scriven, E.F.V., Taylor, R.J.K., Eds.; Elsevier: Oxford, UK, 2008; Volume 6, pp. 257–424.
19. Forkey, D.M.; Carpenter, W.R. Mass spectrometry of methyltetrazoles. *Org. Mass Spectrom.* **1969**, *2*, 433–445. [[CrossRef](#)]
20. Larina, L.I. Chapter Five—Tautomerism and Structure of Azoles: Nuclear Magnetic Resonance Spectroscopy. In *Advances in Heterocyclic Chemistry*; Scriven, E.F.V., Ramsden, A., Eds.; Elsevier: Oxford, UK, 2018; Volume 124, pp. 233–321. [[CrossRef](#)]
21. Frisch, M.J.; Trucks, G.W.; Schlegel, H.B.; Scuseria, G.E.; Robb, M.A.; Cheeseman, J.R.; Scalmani, G.; Barone, V.; Mennucci, B.; Petersson, G.A.; et al. *Gaussian 09, Revision D01*; Gaussian Inc.: Wallingford, CT, USA, 2013.
22. Becke, A.D. Density functional exchange energy approximation with correct asymptotic behavior. *Phys. Rev. A* **1988**, *38*, 3098–3100. [[CrossRef](#)] [[PubMed](#)]
23. Lee, C.; Yang, W.; Parr, R.G. Development of the Colle-Salvetti correlation-energy formula into a functional of the electron density. *Phys. Rev. B Condens. Matter Mater. Phys.* **1988**, *37*, 785–792. [[CrossRef](#)] [[PubMed](#)]
24. Lu, T.; Chen, F. Multiwfn: A multifunctional wavefunction analyzer. *J. Comput. Chem.* **2012**, *33*, 580–592. [[CrossRef](#)] [[PubMed](#)]
25. Merrick, J.P.; Moran, D.; Radom, L. An Evaluation of Harmonic Vibrational Frequency Scale Factors. *J. Phys. Chem. A* **2007**, *111*, 11683–11700. [[CrossRef](#)] [[PubMed](#)]
26. Sheldrick, G.M. SHELXT—Integrated space-group and crystal-structure determination. *Acta Cryst.* **2015**, *A71*, 3–8. [[CrossRef](#)] [[PubMed](#)]
27. Sheldrick, G.M. Crystal structure refinement with SHELXL. *Acta Cryst.* **2015**, *C71*, 3–8. [[CrossRef](#)]
28. Dolomanov, O.V.; Bourhis, L.J.; Gildea, R.J.; Howard, J.A.K.; Puschmann, H. OLEX2: A complete structure solution, refinement and analysis program. *J. Appl. Cryst.* **2009**, *42*, 339–341. [[CrossRef](#)]

Disclaimer/Publisher’s Note: The statements, opinions and data contained in all publications are solely those of the individual author(s) and contributor(s) and not of MDPI and/or the editor(s). MDPI and/or the editor(s) disclaim responsibility for any injury to people or property resulting from any ideas, methods, instructions or products referred to in the content.